Published in final edited form as:
*Nucl Med Biol*. 2011 July ; 38(5): 667–674. doi:10.1016/j.nucmedbio.2010.12.007.

# Analysis of Metabolism of 6FDG: A PET Glucose Transport Tracer

**Raymond F. Muzic Jr.**[1,2], **Visvanathan Chandramouli**[1], **Hsuan-Ming Huang**[2], **Chunying Wu**[1], **Yanming Wang**[1], and **Faramarz Ismail-Beigi**[3]

[1] Department of Radiology, Case Western Reserve University

[2] Department of Biomedical Engineering, Case Western Reserve University

[3] Department of Medicine, Case Western Reserve University

## Abstract

**Introduction—**We are developing $^{18}$F-labeled 6-fluoro-6-deoxy-D-glucose ([$^{18}$F]6FDG) as a tracer of glucose transport. As part of this process it is important to characterize and quantify putative metabolites. In contrast to the ubiquitous PET tracer $^{18}$F-labeled 2-fluoro-2-deoxy-D-glucose ([$^{18}$F]2FDG) which is phosphorylated and trapped intracellularly, the substitution of fluorine for a hydroxyl group at carbon 6 in [$^{18}$F]6FDG should prevent its phosphorylation. Consequently, [$^{18}$F]6FDG has the potential to trace the transport step of glucose metabolism without the confounding effects of phosphorylation and subsequent steps of metabolism. Herein the focus is to determine whether, and the degree to which, [$^{18}$F]6FDG remains unchanged following intravenous injection.

**Methods—**Biodistribution studies were performed using 6FDG labeled with $^{18}$F as well as the longer-lived radionuclides $^{3}$H and $^{14}$C. Tissues were harvested at 1, 6, and 24 h following intravenous administration and radioactivity was extracted from the tissues and analyzed using a combination of ion exchange columns, high-performance liquid chromatography, and chemical reactivity.

**Results—**At the 1 h time-point, the vast majority of radioactivity in the liver, brain, heart, skeletal muscle, and blood was identified as 6FDG. At the 6- and 24-h time-points there was evidence of a minor amount of radioactive materials that appeared to be 6-fluoro-6-deoxy-D-sorbitol and possibly 6-fluoro-6-deoxy-D-gluconic acid.

**Conclusion—**On the time scale typical of PET imaging studies radioactive metabolites of [$^{18}$F]6FDG are negligible.

### Keywords

Glucose transport; 6-fluoro-6-deoxy-D-glucose

Corresponding Author: Raymond F. Muzic, Jr., Department of Radiology, University Hospitals Case Medical Center, 11100 Euclid Avenue, Cleveland, OH 44106, raymond.muzic@case.edu, 216-844-3543.

## 1. Introduction

Glucose entry into cells is facilitated by a family of glucose transporters (GLUTs) [1–3]. Upon entry, glucose is rapidly phosphorylated and metabolized. Glucose analogues such as 2-deoxy-D-glucose (2DG1) and $^{18}$F-labeled 2-fluoro-2-deoxy-D-glucose ([$^{18}$F]2FDG; commonly used for PET scanning) are transported, phosphorylated, and, because they do not readily exit the cell and are not metabolized further, accumulate intracellularly. Hence, these agents measure the sum of both transport and phosphorylation steps of metabolism.

We are developing [$^{18}$F]6-fluoro-6-deoxy-D-glucose ([$^{18}$F]6FDG) as a glucose analog for imaging only the glucose transport step [4–6]. In addition, when used in conjunction with [$^{18}$F]2FDG, rates of both the transport and phosphorylation steps can be individually estimated. Indeed, Bertoldo *et al*. [7,8] have taken a multiple tracer approach for measuring transport and phosphorylation. To do this they used [$^{18}$F]2FDG plus 3-*O*-methyl-glucose (3OMG), a commonly used compound to measure the transport step alone, labeled with $^{11}$C for measurement by PET. We propose that [$^{18}$F]6FDG would be preferred to [$^{11}$C]3OMG as a transport tracer because of the longer half-life of $^{18}$F compared to that of $^{11}$C (110 vs. 20 min) in addition to the favorable biochemical properties of 6FDG as summarized below.

That 6FDG is a substrate for glucose transport has been established. Years ago, prior to the elucidation of glucose transporter families and isoforms, Wilson and Landau [9] demonstrated that 6FDG is actively transported across hamster intestinal sacs. We now attribute this active transport to sodium-dependent glucose transporters (SGLTs), transporters that are near-selectively expressed in the intestine and kidney. Indeed, our recent studies in intact rats demonstrate little urinary excretion of [$^{18}$F]6FDG unless rats are pre-treated with phlorizin, an inhibitor of SGLTs [5]. Moreover, we have established that 6FDG is transported by the facilitative glucose transporters (GLUTs). Specifically, studies in cell culture systems demonstrate that a significant fraction of 6FDG transport can be blocked by cytochalasin B, an inhibiter of GLUTs, in Clone 9 cells that express GLUT1 and in 3T3-L1 adipocytes that express GLUT1 and GLUT4 [5]. In addition, we have demonstrated that insulin, which increases the abundance of GLUT4 transporters in the surface of target cells by causing translocation to the plasma membrane, increases skeletal muscle [$^{18}$F]6FDG concentration by greater than twofold over the fasting state in rats maintained under euglycemic clamp conditions [6]. In particular, we have previously reported normalized [$^{18}$F]6FDG time-activity curves and images in control versus insulin-stimulated states [6] as well as in comparison to [$^{18}$F]2FDG curves and images in control and SGLT-blocked conditions [5]. *A priori* we expected [$^{18}$F]6FDG would be transported by the GLUT facilitative transporters (present in most, if not all, tissues), and that plasma, interstitial, and intracellular concentrations would be nearly equal at later time-points. Hence, we interpreted our early data as being in accord with [$^{18}$F]6FDG distributing in total body water [5]. Subsequently, we found evidence that contradicts this explanation: skeletal muscle radioactivity concentrations in hyperinsulinemia plateau at approximately double that in the control state [6]. This doubling was analogous to that which occurred in human skeletal muscle as probed using the non-metabolized transport tracer [$^{11}$C]3OMG [10]. One potential explanation is this is a consequence of competition between intracellular [$^{18}$F]6FDG and intracellular glucose for efflux mediated by GLUTs [6]: insulin stimulation is known to increase intracellular glucose concentration. Assuming glucose and 6FDG compete with the same transporters for cellular efflux, the increased intracellular glucose concentration would reduce 6FDG efflux so that its intracellular concentration might exceed its interstitial concentration. Another possibility is that insulin could increase perfusion via

[1]We refer to compounds without indicating the radiolabel when considering biochemical properties that are assumed to be independent of the label.

capillary recruitment and open up a greater space to fill with 6FDG. All these interpretations assumed that the majority of tissue radioactivity is due to [$^{18}$F]6FDG itself, and not to its potential radioactive metabolites.

Accordingly, the next step in developing [$^{18}$F]6FDG as a glucose transport tracer is to determine the extent to which 6FDG may be metabolized. Despite prior work showing that various fluorinated glucose analogs are significantly metabolized [11–13], a preliminary evaluation of 6FDG indicated lack of its phosphorylation by hexokinase *in vitro* [6]. This was not too surprising, given that the phosphorylation of glucose by hexokinase occurs on carbon 6 whereas at this position in 6FDG, the substitution of a hydroxyl with fluorine was expected to prevent phosphorylation. Nevertheless, the question of 6FDG metabolism by any pathway has not been thoroughly investigated and thus is the subject of this report.

## 2. Materials and methods

A number of analytical methods were used to determine whether and the degree to which 6FDG remains unchanged following intravenous injection and to identify, to the extent practicable, the most significant metabolites.

### 2.1 Subjects

Female Sprague-Dawley rats were purchased from Charles River Laboratories International and housed in the ALAC-accredited Animal Research Center at Case Western Reserve University. Females were used to facilitate urinary catheterization. Normal husbandry included access to food and water and a daily 12 h on-off light-cycle. In the afternoon prior to the study food was removed and animals fasted overnight. The animal protocol was reviewed and approved by the Institutional Animal Care and Use Committee (IACUC) of Case Western Reserve University. Animal care was supervised by veterinarians and the IACUC and adheres to the NIH Guidelines for Lab Animal Care and the Animal Welfare Act.

### 2.2 [$^{18}$F]6FDG Experiments

The biodistribution and chemical properties of radioactivity, either 1 or 6 h after tail vein injection of [$^{18}$F]6FDG were evaluated. On mornings of the experiments, [$^{18}$F]6FDG was synthesized using a modification of a previously reported procedure [4,6]. The final product was obtained with purification by HPLC to achieve greater than 99% radiochemical purity. Rats were anesthetized using 2% isoflurane in oxygen and [$^{18}$F]6FDG injected into tail vein. To achieve satisfactory radioactivity concentrations for the analytical methods and considering the 110 minute half-life of $^{18}$F, approximately 37 MBq (1 mCi) and 370 MBq (10 mCi) were injected into the rats used for the 1 and 6 h time points, respectively. For the rats used for the 1 h time point, a urinary catheter (PE10, 0.28 mm ID, 0.61 mm OD) was placed and used to collect urine [14] while the rat remained anesthetized until euthanasia by decapitation at 1 h. Following injection, rats used for the 6 h time point were placed in a metabolic cage and allowed to recover from anesthesia. Then, approximately 15 minutes prior to euthanasia, rats were anesthetized again. Rats, for both time points, were heparinized (1000 U/kg), prior to euthanasia to facilitate blood collection.

### 2.3 Tissue Collection and Processing

Immediately following euthanasia, blood was collected in a heparinized beaker and the carcass was dissected. Freshly harvested tissues were promptly weighed, minced, and transferred to tubes containing 8 mL/g of ice-cold ethanol:PBS:water buffer (65:10:25, vol:vol:vol) [15], and then homogenized (Tissue Homogenizer, Model TH, Omni International, Kennesaw, GA). Homogenates were centrifuged for 15 min at 23,500 × g and

4° C (Sorvall RC 5C Plus with SS-34 rotor, Thermo Scientific, Waltham, MA). Supernatants were collected and volumes noted. Aliquots, 0.1 mL, of supernatants were taken to determine radioactivity using a well-counter with a NaI(Tl) crystal (LKB-Wallac, Compu-Gamma 1282, Turku, Finland). Lipids were removed by extraction with chloroform:methanol (2:1, vol:vol). For this, 2 mL aliquots of homogenate supernatants were evaporated to dryness, reconstituted in 2 mL of water, and 7 mL of 2:1 chloroform:methanol was added. Samples were mixed and then centrifuged at 12,000 × g for 10 min. The top layer containing methanol and water was carefully removed, evaporated, and reconstituted with 2 mL water. A 0.1 mL aliquot of this was counted to determine radioactivity. The remaining 1.9 mL was analyzed for charged metabolites using ion exchange columns as described below. Heparinized blood was evaluated by diluting it five-fold in water to hemolyze cells. Zinc sulfate (Sigma-Aldrich, Co., St. Louis, MO), 0.3 N, was added, 2 mL/mL blood; the samples mixed; barium hydroxide (Sigma-Aldrich, Co.), 0.3 N, added, 2 mL/mL blood; samples mixed again; and then centrifuged at 23,500 × g for 15 min to precipitate proteins [16]. Supernatants were removed and assayed for radioactivity. Radioactivity in urine was directly measured.

### 2.4 Ion Exchange Colum Analysis

After reconstitution in water, radioactivity from the methanol-water layer was passed down an anion exchange column in the formate form (AG 1-X8 resin, 100–200 mesh, Bio-Rad, Hercules, CA). The column was eluted with 10 mL water which was collected in two fractions. To release bound, negatively charged material, the column was rinsed with 10 mL of 4 N formic acid which was collected in two fractions. Eluates and the columns themselves were counted.

### 2.5 [1-$^{3}$H]6FDG Experiments

Studies were conducted using [1-$^{3}$H]6FDG since the longer half-life of $^{3}$H than that of $^{18}$F facilitated additional analyses. [1-$^{3}$H]6FDG was prepared from [1-$^{3}$H]glucose as described previously [5]. Animal handling was similar to that performed using [$^{18}$F]6FDG with the following differences. 74 kBq (2 μCi) of [1-$^{3}$H]6FDG was injected. In addition to the 1 and 6 h time points, 24-h time points were also acquired.

Tissue homogenates, again prepared in ice-cold ethanol-PBS-water buffer, were centrifuged at 7,500 × g (Sorvall Superspeed RC2-B with SS-34 rotor) at 4° C and supernatants decanted and filtered. 1-mL aliquots were taken for total radioactivity determination using a Packard Tri-Carb 1600 (PerkinElmer, Waltham, MA) liquid scintillation counter with 15 mL of EcoLume scintillation fluid (ICN Biomedicals, Costa Mesa, CA) per mL of sample.

Blood filtrates and tissue homogenates were further analyzed to evaluate potential charged metabolites. 5-mL aliquots of blood filtrates were evaporated to dryness, reconstituted in 2 mL water and then directly applied to the anion exchange columns. Columns were washed first with 25 mL of water and then with 10 mL of 4 N formic acid. Aliquots of eluates were assayed for radioactivity. Dried tissue homogenates were reconstituted in 4 mL water and lipids were extracted using chloroform-methanol as described above. The methanol-water layer was carefully collected, evaporated, and reconstituted in 2 mL of water. A 0.1-mL aliquot was assayed for radioactivity and extraction efficiency was determined as the ratio of radioactivity obtained in the methanol-water layer to that in homogenate. The remaining 1.9 mL was analyzed for negatively charged compounds using an anion exchange column. Water-wash eluates were additionally analyzed for positively charged compounds using cation ($H^{+}$) exchange columns (AG50W-X8 resin 100–200 mesh, Bio-Rad) eluted with 20 mL. Aliquots of washes were assayed for radioactivity. To evaluate neutral compounds, the remainder of the water washes were evaporated, reconstituted in 1 mL of water, and then

analyzed by HPLC using an Aminex lead column (HPX-87P, Bio-Rad) maintained at 80° C. The flow rate was set to 0.5 mL/min and water used as the eluent. Eulate fractions were collected and assayed for radioactivity. Results were compared to times of elution of 6FDG and 6-fluoro-6-deoxy-D-sorbitol (6FDS) standards.

Chemical reactivity was used to test if the HPLC fraction that eluted with the retention time of the 6FDS standard also reacts as 6FDS. Specifically, samples were evaluated by measuring radioactivity converted to formal dimedon [17]. This provides a means to specifically identify [1-$^{3}$H]6FDS in the HPLC fractions since [1-$^{3}$H]6FDS should react quantitatively whereas [1-$^{3}$H]6FDG should remain unchanged. To confirm this behavior, [1-$^{3}$H]6FDG and [1-$^{3}$H]6FDS standards were also analyzed.

### 2.6 [U-$^{14}$C]6FDG Experiments

To assess the possibility of metabolic de-tritiation of [1-$^{3}$H]6FDG and the potential to significantly underestimate metabolites when using [1-$^{3}$H]6FDG, we also performed studies using [U-$^{14}$C]6FDG as the labeled backbone of the molecule would mean potential metabolites would be labeled. Specifically, radioactivity biodistribution was evaluated 1 and 6 h following co-administration of 74 kBq (2 μCi) of [1-$^{3}$H]6FDG and 56 kBq (1.5 Ci) of [U-$^{14}$C]6FDG. [U-$^{14}$C]6FDG was prepared from [U-$^{14}$C]glucose analogously to the preparation of [1-$^{3}$H]6FDG from [1-$^{3}$H]glucose. Using liquid scintillation counting with appropriate energy windows, $^{14}$C and $^{3}$H activities were measured in the aliquots of supernatants of homogenates prior to and following evaporation and reconstitution in buffer. Results were expressed as percent of radioactivity in aliquots of homogenates after vs. before evaporation. These percentages were statistically analyzed after log-transformation, to improve the normality of the data, and averaging across 6 tissues in each of 3 animals per time point. The resulting values were compared to zero by the one-sample t-test. (In absence of loss, the percentage would be 100% and its logarithm would be zero.)

## 3 Results

### 3.1 Extraction efficiency of $^{18}$F radioactivity

Figure 1 shows the percentage of homogenate $^{18}$F radioactivity that is present in the methanol-water layer obtained in the lipid extraction procedure. Each data point summarizes results from 3 animals each at 1 or 6 hours. Overall, average extraction from all tissues was 95.6 ± 2.6% for 1 h and 90.5 ± 2.6% for 6 h suggesting there was a minor amount of radioactivity trapped, perhaps in lipids. Conversely, greater than 90% of the radioactivity in the homogenates was recovered in the methanol-water phase indicating that any potential major metabolite would be revealed in our analyses.

### 3.2 Chemical Composition of Extracted $^{18}$F Radioactivity

Figure 2 summarizes results of anion exchange column analysis of radioactivity extracted in the methanol-water phase. Values were expressed according to the percentage of the applied $^{18}$F radioactivity that a) eluted with water, b) eluted with 4 N formic acid, or c) remained bound to the column. 6FDG and neutrally charged metabolites, if any were present, should appear in the water eluate. Negatively charged metabolites such as phosphates should elute with formic acid. In all tissues, the majority of the radioactivity eluted with water. The formic acid eluate fractions tended to be higher at 6 h than 1 h, ranging from 11 to 22% at 6 h vs. 2 to 9% at 1 h, suggesting the formation of minor amounts of one or more negatively charged metabolites. In general, little radioactivity remained bound to the column for all tissues except liver which demonstrated a time-dependent increase from 1% at 1 h to 5% at 6 h.

### 3.3 [1-$^{3}$H]6FDG Experiments

Figure 3 shows results of ion exchange column analysis of $^{3}$H radioactivity extracted from homogenates of animals injected with [1-$^{3}$H]6FDG and which appeared in the methanol-water layer. In this extension of the experiments using $^{18}$F shown in Figure 2, the longer half-life of $^{3}$H than that of $^{18}$F facilitates analyses using both anion- (Figure 3A) and cation-exchange (Figure 3B) columns, as well as inclusion of a 24-h time point. In general, results using anion exchange columns on extracts from animals injected with [1-$^{3}$H]6FDG were similar with those from animals injected with [$^{18}$F]6FDG (noted above) in that at the 1-h time point, there was no clear evidence of metabolites: approximately 90% or more of the radioactivity eluted with water and for all tissues the difference from 100% was less than one standard deviation and the average across tissues being 101%. For the 6-h and 24-h time-points, the averages across tissues indicated 94% and 95% of radioactivity eluting with water, with the results being somewhat variable. The only tissue that demonstrated a clear decreasing trend over time was skeletal muscle. As for the cation exchange column results, there was no clear indication of positively charged metabolites since the percentage of radioactivity eluting with water was close to 100% and was not systematically decreasing with time, Figure 3B.

### 3.4 HPLC Results with [1-$^{3}$H]6FDG

Figure 4 shows representative HPLC traces of water eluates from the anion exchange column which should contain [1-$^{3}$H]6FDG and uncharged metabolites if any were present. In blood, virtually all the radioactivity eluted as a single peak with a retention time matching that of the [1-$^{3}$H]6FDG standard. With brain and heart, the majority of the radioactivity eluted in the same peak however there were secondary peaks with retention times matching that of the [1-$^{3}$H]6FDS standard. In general, the [1-$^{3}$H]6FDG peaks were lower and the [1-$^{3}$H]6FDS peaks were higher at the later vs. earlier time points, consistent with metabolism.

### 3.5 HPLC Quantification

HPLC results were quantified according to the percent of radioactivity in each peak. Results are shown in Figure 5. The trend indicated a reduction in the percentage of [1-$^{3}$H]6FDG at the later biodistribution time-points. The tissues with the lowest percentage of radioactivity eluting as 6FDG at 1, 6, and 24 h, respectively were heart (90%), heart (69%), and skeletal muscle (65%). The tissues with the highest percentage of radioactivity eluting as [1-$^{3}$H]6FDS were heart (18%), heart (28%), and skeletal muscle (31%) at these respective time points. Although blood was not obtained in the 24 h data set, essentially all (> 99%) of is radioactivity eluted as [1-$^{3}$H]6FDG at 6 h.

### 3.6 Dimedon

In control experiments conducted using standards, formal dimedon had 0.1% of the radioactivity with [1-$^{3}$H]6FDG and 93% with [1-$^{3}$H]6FDS, indicating [1-$^{3}$H]6FDG reacts negligibly and [1-$^{3}$H]6FDS reacts almost completely. Quantitative conversion of the metabolite fraction to formal dimedon which contained 95 ± 0.1 % and 90 ± 4.8% of the radioactivity from the fractions obtained from skeletal muscle and heart, respectively, provides additional evidence that the fraction that eluted like 6FDS was indeed 6FDS.

### 3.7 Loss of $^{3}$H from [1-$^{3}$H]6FDG Metabolism

Activities of homogenates, before and after evaporation, were measured to test the possibility of loss of the $^{3}$H label by metabolic detritiation. Results, expressed as percent of radioactivity remaining after evaporation, are shown in Figure 6. For animals euthanized 1 h after injection, natural logarithms of the radioactivity ratios were 0.0097 ± 0.0072 (mean ±

SD) for $^{3}$H and 0.0289 ± 0.0192 for $^{14}$C with respective p-values of 0.15 and 0.12 indicating no statistically significant loss of radioactivity by evaporation. For animals euthanized 6 h after injection, natural logarithms of ratios were −0.189 ± 0.015 for $^{3}$H and 0.0148 ± 0.0211 for $^{14}$C with respective p-values of 0.001 and 0.35 indicating significant loss of $^{3}$H, but not $^{14}$C, with evaporation.

### 3.8 Radioactivity Excreted in Urine

Urinary excretion of radioactivity over 1, 6 and 24 h is shown in Figure 7. Due to the short half-life of $^{18}$F, only $^{3}$H data are available for the 24 time point. Overall the data demonstrate low excretion indicative of good reabsorption of 6FDG by the kidneys.

## 4. Discussion

The efficiency of extraction of radioactivity in homogenates was in excess of 90%, Figure 1, confirming that, should there be any, major metabolites would be revealed in the subsequent biochemical analyses. In the initial analysis, we used anion exchange columns to test for negatively charged metabolites, such as phosphates, which would be present if 6FDG were metabolized similarly to glucose; negatively charged metabolites would be retained on the column when rinsed with water and be eluted with formic acid. Considering the data from the 1 h biodistribution time point, the appearance of greater than 89% $^{18}$F radioactivity in the water eluates and less than 10% in the formic acid eluates, Figure 2, indicates there are few negatively charged metabolites. The overall trend for few negatively charged metabolites was similar with [1-$^{3}$H]6FDG, Figure 3. Moreover, the cation exchange column results at the 1-h biodistribution time showed essentially 100% of the $^{3}$H radioactivity eluting with water indicating lack of positively charged metabolites. Further, because both the HPLC analysis and dimedon reactivity assay indicate the majority of radioactivity in the water eluates behaves as 6FDG, we must conclude that at the 1 h biodistribution time, radioactivity is nearly all 6FDG and that the amount of metabolites that would be present during the time-scale of a PET scan would be negligible. Additional support for this conclusion is found in the low urinary excretion of radioactivity and the particularly high percentage of blood radioactivity that behaved as 6FDG.

At the later 6-h time point we observed evidence of a non-negligible amount of metabolites with HPLC and dimedon results suggesting the presence of 6FDS. We speculate that 6FDG could be reduced by aldose reductase given that this enzyme seems to be able to reduce other fluorinated glucose analogs such as 3FDG to 3-fluoro-3-deoxy-D-sorbitol [12]. Whereas Berkowitz *et al.* [12] observed subsequent metabolism of 3-fluoro-3-deoxy-D-sorbitol to 3-fluoro-3-deoxy-fructose, we found no evidence of 6FDS being metabolized to 6-fluoro-6-deoxy-fructose: the HPLC traces showed no additional peak between those of 6FDG and 6FDS.

We speculate that 6-fluoro-6-deoxy-D-gluconic acid might be a minor metabolite formed by oxidation of 6FDG which could be catalyzed by glucose dehydrogenase as occurred with 3FDG [12]. In skeletal muscle in particular, we observed a time-dependent increase in radioactivity that was retained on the anion exchange column after rinsing with water and released by rinsing with formic acid. Moreover, at 6 h we found a small but statistically significant loss of $^{3}$H from its position on carbon 1 with [1-$^{3}$H]6FDG. This could be explained by glucose dehydrogenase catalyzing oxidation of [1-$^{3}$H]6FDG to form 6-fluoro-6-deoxy-D-gluconic acid with release of $^{3}$H. Indeed, glucose dehydrogenase, derived from rat liver, exhibited the same activity on D-glucose, 6-fluoro-D-glucose, and 6-deoxy-D-glucose indicating that the hydroxyl on carbon 6 is probably not necessary for oxidation by glucose dehydrogenase [18]. Further, when glucose dehydrogenase acted on glucose, the product behaved as gluconate, the anionic form of gluconic acid [18].

Urinary excretion data indicated that by 24 h, less than 8% of the radioactivity was excreted. This is much less than the 50% excretion reported for 3OMG by 5 h [19,20] and suggests that 6FDG is a better substrate for the SGLTs than is 3OMG. Indeed, [$^{18}$F]6FDG might be particularly useful for evaluating strategies to block SGLT2 in an effort to manage blood glucose levels.

In summary, we find 6FDG to undergo minimal metabolism over the time durations used for PET scanning. The metabolites that appear to be formed, 6FDS and 6FGA, are analogous to those formed with 3FDG although the amounts with 6FDG are much lower. Although 3OMG is widely believed to be inert, at least one paper reports that it can be phosphorylated and subsequently dephsophorylated in rat heart [21] and one reports it can be phosphorylated *in vitro* by hexokinase [22]. Moreover, 3OMG can be labeled with $^{11}$C but not $^{18}$F and so has a much shorter radioactive half-life than [$^{18}$F]6FDG. Thus we conclude [$^{18}$F]6FDG may be the preferred compound for imaging glucose transport with PET.

## Acknowledgments

We thank William C Schumann, PhD for synthesis of the [U-$^{14}$C]- and [1-$^{3}$H]6FDG and the precursor for making [$^{18}$F]6FDG. We thank Mark D Schluchter for advice on statistical analysis. This work was supported by grant R01 DK082423 from the National Institutes of Health, National Institute of Diabetes and Digestive and Kidney Diseases.

## Abbreviations

| | |
|---|---|
| **6FDG** | 6-fluoro-6-deoxy-D-glucose |
| **6FDS** | 6-fluoro-6-deoxy-D-sorbital |
| **6FGA** | 6-fluoro-6-deoxy-D-gluconic acid |

## Bibliography

1. Lodish, H.; Berk, A.; Matsudaria, P.; Kaiser, CA.; Krieger, M.; Scott, MP.; Zipursky, SL.; Darnell, J. Molecular Cell Biology. 5. 2004.
2. Helmke BM, Reisser C, Idzko M, Dyckhoff G, Herold-Mende C. Expression of SGLT-1 in preneoplastic and neoplastic lesions of the head and neck. Oral Oncol. 2004; 40(1):28–35. [PubMed: 14662412]
3. Scheepers A, Joost HG, Schurmann A. The glucose transporter families SGLT and GLUT: molecular basis of normal and aberrant function. JPEN J Parenter Enteral Nutr. 2004; 28(5):364–371. [PubMed: 15449578]
4. Neal TR, Schumann WC, Berridge MS, Landau BR. Synthesis of [$^{18}$F]-deoxy-d-fluoro-D-glucose ([$^{18}$F]6FDG), a potential tracer of glucose transport. Journal of Labelled Compounds and Radiopharmaceuticals. 2005; 48(11):845–854.
5. Landau BR, Spring-Robinson CL, Muzic RF Jr, Rachdaoui N, Rubin D, Berridge MS, Schumann WC, Chandramouli V, Kern TS, Ismail-Beigi F. 6-Fluoro-6-deoxy-D-glucose as a tracer of glucose transport. Am J Physiol Endocrinol Metab. 2007; 293(1):E237–E245. [PubMed: 17405828]
6. Spring-Robinson C, Chandramouli V, Schumann WC, Faulhaber PF, Wang Y, Wu C, Ismail-Beigi F, Muzic RF Jr. Uptake of 18F-labeled 6-fluoro-6-deoxy-D-glucose by skeletal muscle is responsive to insulin stimulation. J Nucl Med. 2009; 50(6):912–919. [PubMed: 19443592]
7. Bertoldo A, Price J, Mathis C, Mason S, Holt D, Kelley C, Cobelli C, Kelley DE. Quantitative assessment of glucose transport in human skeletal muscle: dynamic positron emission tomography imaging of [O-methyl-$^{11}$C]3-O-methyl-D-glucose. J. Clin. Endocrinol Metab. 2005; 90(3):1752–1759.

8. Bertoldo A, Pencek RR, Azuma K, Price JC, Kelley C, Cobelli C, Kelley DE. Interactions between delivery, transport, and phosphorylation of glucose in governing uptake into human skeletal muscle. Diabetes. 2006; 55(11):3028–3037. [PubMed: 17065339]
9. Wilson TH, Landau BR. Specificity of sugar transport by the intestine of the hamster. Am J Physiol. 1960; 198:99–102. [PubMed: 13845137]
10. Pencek RR, Bertoldo A, Price J, Kelley C, Cobelli C, Kelley DE. Dose-responsive insulin regulation of glucose transport in human skeletal muscle. Am J Physiol Endocrinol Metab. 2006; 290(6):E1124–E1130. [PubMed: 16390860]
11. Halama JR, Gatley SJ, DeGrado TR, Bernstein DR, Ng CK, Holden JE. Validation of 3-deoxy-3-fluoro-D-glucose as a glucose transport analogue in rat heart. Am J Physiol. 1984; 247(5 Pt 2):H754–H759. [PubMed: 6496756]
12. Berkowitz BA, Moriyama T, Fales HM, Byrd RA, Balaban RS. In vivo metabolism of 3-deoxy-3-fluoro-D-glucose. J Biol Chem. 1990; 265(21):12417–12423. [PubMed: 2115519]
13. Gatley SJ. Labeled glucose analogs in the genomic era. J Nucl Med. 2003; 44(7):1082–1086. [PubMed: 12843225]
14. Waynforth, HB.; Flecknell, PA. Experimental and Surgical Techniques in the Rat. 2. San Diego: Academic Press; 1992. p. 36-39.
15. Dienel GA, Cruz NF, Mori K, Sokoloff L. Acid lability of metabolites of 2-deoxyglucose in rat brain: implications for estimates of kinetic parameters of deoxyglucose phosphorylation and transport between blood and brain. J Neurochem. 1990; 54(4):1440–1448. [PubMed: 2156023]
16. Somogyi M. Determination of Blood Sugar. J Biol Chem. 1945; 160:69–73.
17. Reeves RR. The estimation of primary carbinol groups in carbohydrates. J Am Chem Soc. 1941; 63(5):1476–1477.
18. Metzger RP, WILCOX SS, WICK AN. Studies with rat liver glucose dehydrogenase. J Biol Chem. 1964; 239:1769–1772. [PubMed: 14213348]
19. Lang JA, Gisolfi CV, Lambert GP. Effect of exercise intensity on active and passive glucose absorption. Int J Sport Nutr Exerc Metab. 2006; 16(5):485–493. [PubMed: 17240781]
20. Zuckerman MJ, Menzies IS, Ho H, Gregory GG, Casner NA, Crane RS, Hernandez JA. Assessment of intestinal permeability and absorption in cirrhotic patients with ascites using combined sugar probes. Dig Dis Sci. 2004; 49(4):621–626. [PubMed: 15185867]
21. Gatley SJ, Holden JE, Halama JR, DeGrado TR, Bernstein DR, Ng CK. Phosphorylation of glucose analog 3-O-methyl-D-glucose by rat heart. Biochem Biophys Res Commun. 1984; 119(3): 1008–1014. [PubMed: 6712659]
22. Halseth AE, Bracy DP, Wasserman DH. Limitations to basal and insulin-stimulated skeletal muscle glucose uptake in the high-fat-fed rat. Am J Physiol Endocrinol Metab. 2000; 279(5):E1064–E1071. [PubMed: 11052961]

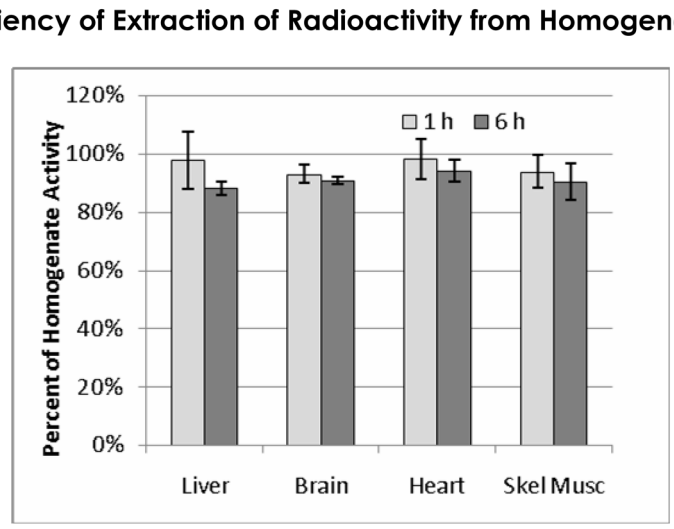


**Figure 1.**

Percentage of radioactivity recovered from homogenates using the lipid extraction procedure. The methanol-water layer had 95.6 ± 2.6% at 1 h and 90.8 ± 2.5% at 6 h of homogenate radioactivity.

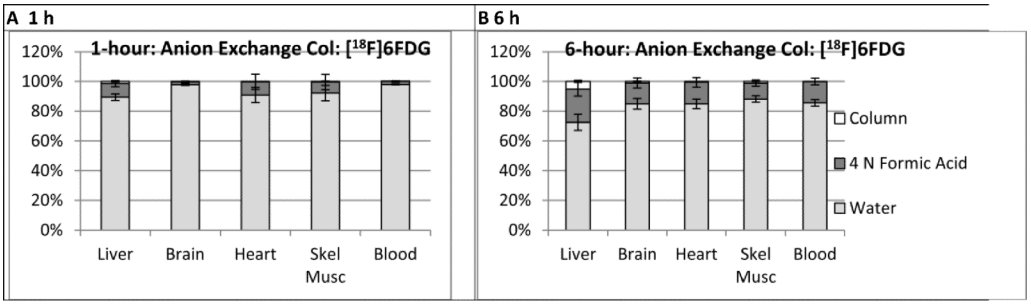


**Figure 2.**

Results of anion exchange column analysis of extracts of homogenates from tissues harvested following intravenous injection of [$^{18}$F]6FDG. For all tissues and both time-points, the majority of radioactivity eluted through the column with water indicating radioactivity is in the form of 6FDG or other neutral compounds. The small percentage of the radioactivity eluted with formic acid, 2 to 9% at 1 h and 11 to 22% at 6 h, implies potential of minor metabolism of [$^{18}$F]6FDG to negatively charged compound(s). Counting the columns following the elutions confirmed all of the radioactivity from the columns was recovered for all tissues except liver in which 1 and 5% remained bound to the column from the 1 h and 6 h data, respectively.

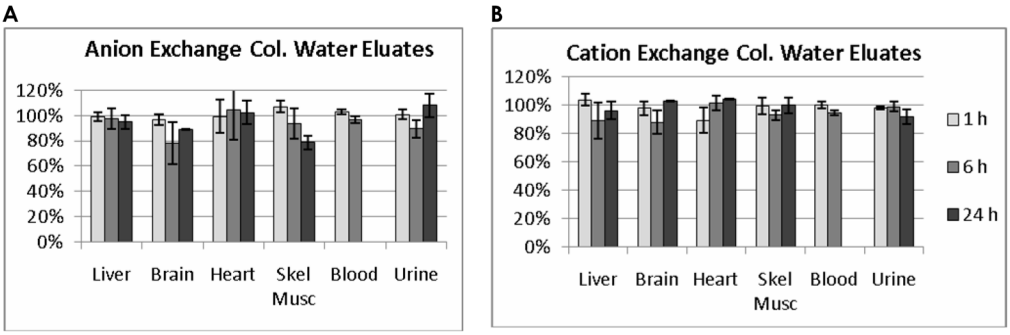


**Figure 3.**

Results of anion and cation exchange column analyses of extracts of homogenates from tissues harvested following intravenous injection of [1-$^{3}$H]6FDG. Extracts of homogenates revealed little evidence of charged metabolites. With the anion exchange column, A, water eluted the majority of the radioactivity indicating lack of negatively charged metabolites (e.g. phosphorylated 6FDG). With the cation exchange column, B, water eluted the majority of the radioactivity indicating lack of positively charged metabolites. Blood radioactivity was negligible at 24 h. Some error bars are too small to be visualized.

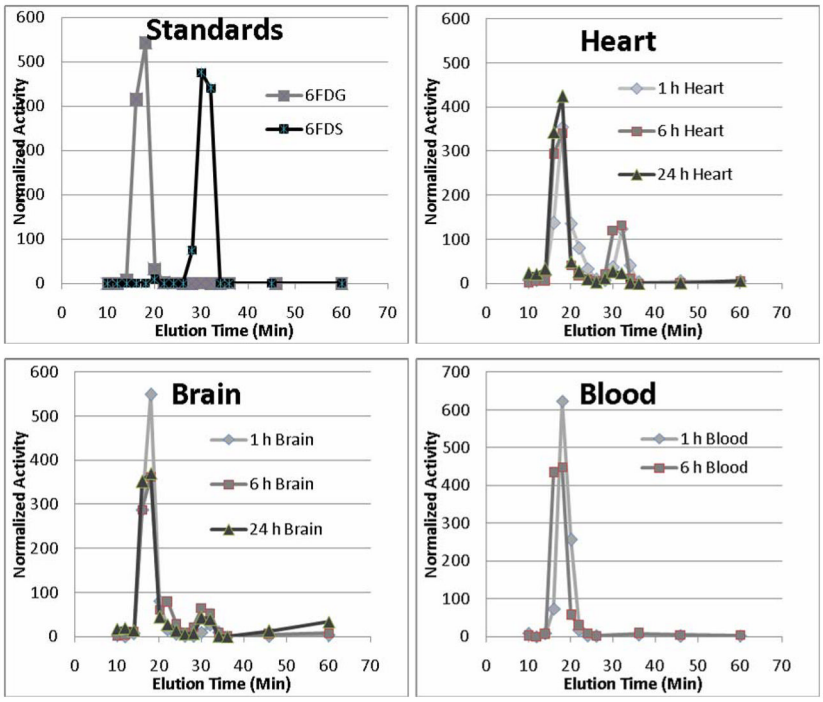


**Figure 4.**

Example HPLC traces from water eluates of anion exchange columns in the [1-$^{3}$H]6FDG experiments. The peak activities from [1-$^{3}$H]6FDG and [1-$^{3}$H]6FDS standards appeared in the fractions collected at 18 and 30 minutes, respectively. In all tissues, the majority of radioactivity eluted at 18 minutes while some tissues exhibited a minor peak at 30 minutes, particularly with the later biodistribution time-points.

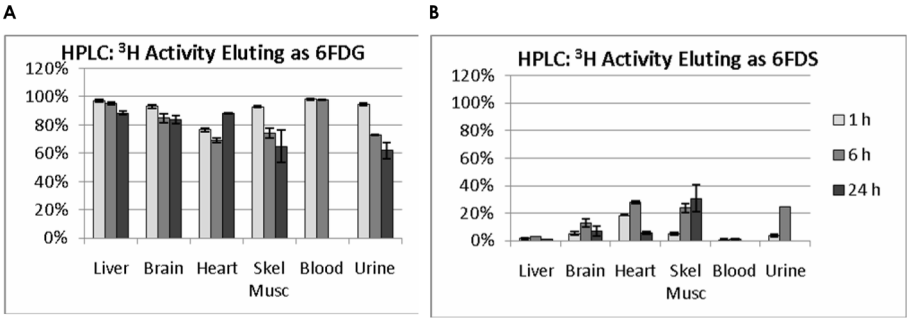


**Figure 5.**

HPLC traces quantified according to the percentage of radioactivity eluting as 6FDG and 6FDS. The radioactivity eluting as 6FDG, A, was high at 1 h and tended to decrease over time. The inverse was true of radioactivity eluting as 6FDG suggesting conversion of 6FDG to 6FDG as a minor metabolic pathway.

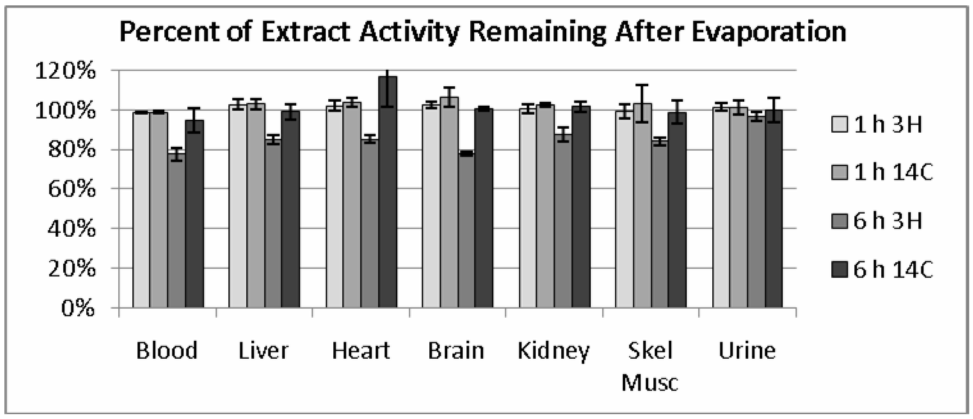


**Figure 6.**

Results of evaporation of homogenates from [1-$^{3}$H]6FDG and [U-$^{14}$C]6FDG experiments. In the 6 h data point, there was a statistically significant loss of $^{3}$H, but not $^{14}$C, with evaporation indicative of loss of $^{3}$H from carbon 1 that could be the consequence of metabolic detritiation.

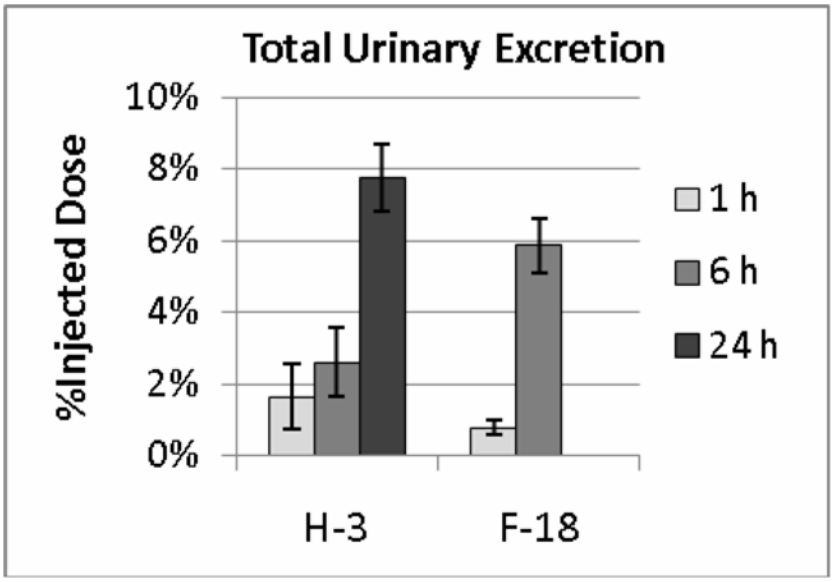


**Figure 7.**
Urinary excretion of radioactivity expressed as a percentage of injected radioactivity. Less than 8% of the $^{3}H$ radioactivity was excreted in 24 h and even less $^{18}F$ and $^{3}H$ radioactivity was excreted at earlier time points. This is consistent with prior data indicating that 6FDG is reabsorbed by sodium-dependent glucose transporters.